2019 IEEE 15th International Conference on Automation Science and Engineering (CASE)

Optical In-Situ Verification of 3D-Printed Electronic Circuits

Florens Wasserfall, Daniel Ahlers, and Norman Hendrich
Computer Science Department, University of Hamburg, Germany
{wasserfall,ahlers,hendrich}@informatik.uni-hamburg.de

***Abstract*— With 3D-Printing becoming a mainstream technology in industry, the need for online process inspection and quality control arises. In this paper, we propose an approach for optical inspection of fused deposition modeling (FDM) printing with integrated electronics. Our prototype setup combines a traditional FDM extruder with an additional extruder for conductive ink, a vacuum pick-and-place nozzle, and two cameras for object alignment and process control. We describe the camera setup, show typical printing faults encountered on our system, and explain our computer vision algorithms to detect (and repair) those faults. We also describe the integration of the inspection modules into existing slicing- and 3D-print-software.**

I. Introduction

Additive manufacturing, and especially the FDM process, continues to gain attention in both the research and the commercial sectors in recent years. Despite a general trend to more precise machines and more robust processes, quality control of the manufactured parts remains a major challenge, and visual inspection methods combined with machine learning classification have been proposed for checking and verifying the geometric properties of the printed objects.

In this paper, we present the design of a computer vision system and the related software for in-situ verification of 3D-printed electronics. Our software records, aligns, and stitches images from every printed layer, then runs computer vision algorithms to segment and classify the image into regions related to the individual extruders. Image regions are then compared with known geometries from the G-code, resulting in automatic detection of defects and possible user-interaction to continue the print (Fig. 1 and 2).

The rest of the paper is structured as follows. First, Sec. II lists the related work for this topic. Sec. III introduces our approach to 3D-printed electronics and describes the details of our custom direct-writing FDM printer. Sec. IV then explicates common problems with the process and the need for in-situ monitoring of the printing progress. Sections V describes the camera setup and the basic computer vision pipeline including robust image stitching and exposure control. Still, the use of different (e.g. color) FDM filaments make static image classification impossible. Therefore, we use machine learning techniques for robust detection and classification of plastic extrusions and conductive traces in Sec. VI. The actual detection of defects in the classified image is described in Sec. VII. Our paper concludes with a summary and an outlook on future work.

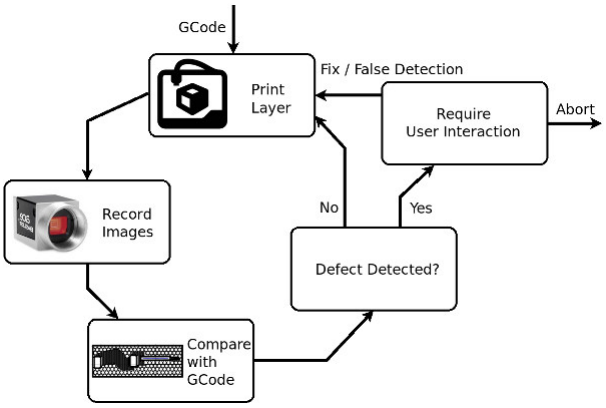

Fig. 1. Workflow of the proposed 3D-printed electronics quality control process. The G-code for our machine combines plastic extrusion, conductive ink extrusion, and pick-and-place commands for SMD electronics components. Once a layer has been completed, a set of images is recorded and stitched together, classified into categories (electronics, ink, plastics) and compared with the expected geometries to detect possible defects.

II. Related Work

The integration of electric connections and electronic components into additively manufactured parts is considered a key feature for applications such as smart devices, wearable devices, or (soft)-robotics. Direct writing of conductive, polymer-based silver inks has been successfully demonstrated for several technologies, including SLA [1], [2] and FDM [3], [4], [5]. A comprehensive review is given by [6].

Optical inspection techniques are a key to quality control for electronics production, and have been researched for

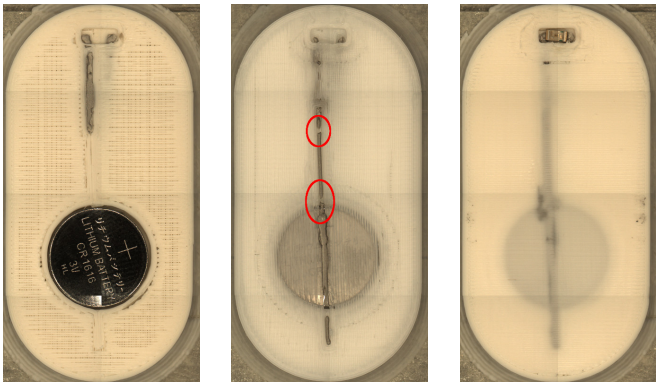

Fig. 2. Three subsequent layers of a 3D-printed give-away flashlight with integrated battery and LED photographed layer-by-layer during print time. The center image highlights typical defects which are not detectable anymore already on the following layer.

978-1-7281-0355-6/19/$31.00 ©2019 IEEE

Fig. 3. Hardware setup used to print objects with integrated electronics. From left to right: **a:** modified RepRap Industrial printer, equipped with **b:** two cameras for component handling and process monitoring, one mounted at the printhead, one next to the printbed **c:** a screw-driven conductive paste extruder and **d:** a rotating vacuum gripper for automatic component placement.

many years; see [7] and [8] for reviews. Full taxonomies of typical faults in conventional PCB manufacturing have been proposed, and most such faults can be detected by computer vision methods, including drill-point defects [9], line-defects [10], defects on PCB inner layers [11], quality of SMD solder dots [12], and SMD components placement [13]. Defects on other materials have been studied as well, e.g. [14] describes a vision system to detect cracks, bubbles, and edge defects on touch-panel glass.

Visual inspection for additive manufacturing has attracted some recent research [15], [16], [17]. Often, machine learning approaches are also included for process control and optimization [18], [19], [20]. Multi-material 3D printing under vision control is described in [21]. In aerosol jet printing, the deposition quality of conductive traces is monitored with cameras [22], and their electrical resistance is estimated with shape-from-shading [23].

The functionality of a printed part can be ensured with the certify-as-you-build paradigm [24], where the quality of a part is ensured by a physical model, in-process sensing, and analysis of this data. In our work, we use the last two of these steps to ensure the quality of the printed circuit.

In our application, even very thin plastic residuals can disrupt the conductive ink direct writing. Therefore, our visual process inspection needs very high-resolution images, difficult to obtain within a single image. Instead, we rely on stitching and tiling of multiple smaller images [25], [26], [27]. Both auto-correlation and feature-based alignment techniques [28], [29], [30] can reach the sub-pixel accuracy required for the task.

III. 3D-printed Electronics in FDM

Figure 3 shows the hardware setup we use to print and assemble fully integrated 3D-electronics. The printer is a modified Kühling&Kühling FDM-printer [31] with a heated chamber for warp-free printing and controlled thermal ink curing. It is augmented with a screw-driven extruder for direct writing of conductive silver ink (Fig. 3 c) and a vacuum gripper to automatically place SMD-components during a print job (Fig. 3 d). Two industrial cameras were added to align the position of electronic components during the pick and place process and for self-calibration of the printer (Fig. 3 b). One camera ("*bed*") is attached to the fixed frame, next to the printbed, facing upwards to take images of SMD-components hold by the vacuum gripper. The second camera ("*head*") is mounted at the x-carriage next to the plastic extruder, facing downwards. It can be positioned at any position within the build-volume, and is used to take the partial images which are then stitched into the full high-res images for layer-by-layer process monitoring.

Figure 4 shows the spatial arrangement and wiring of circuits inside or at the surface of 3D-objects using our modified version [32] of the popular Slic3r slicing software [33]. The result is a standard G-code file which is directly uploaded to the printer. The extrusion traces for conductive wires are encoded as regular `G1` commands for the `T1` tool (`T0` is the plastic extruder). Both cameras are controlled by OctoPNP, an Octoprint plugin for closed loop pick-and-place of SMD-components [34]. OctoPNP exposes an interface which allows other Octoprint plugins to take pictures at given coordinates in the printer.

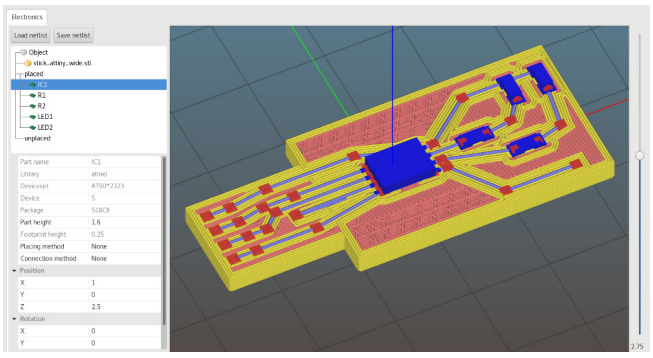

Fig. 4. Screenshot of our custom slicing tool with integrated positioning and wiring of electronic components.

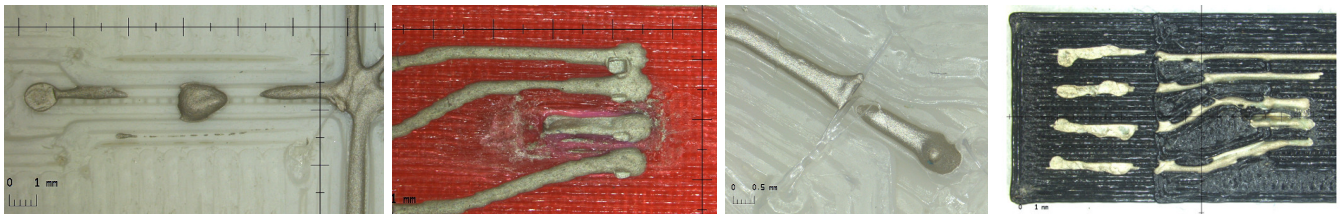

Fig. 5. Typical defects occurring during direct writing of conductive inks on FDM-printed surfaces. From left to right: **1**: insufficient extrusion, **2**: electric short caused by overextrusion, **3**: trace interrupted by plastic string (oozing effect) and **4**: extrusion interrupted by constricted channel exit.

IV. Problem Statement

Today, most electronic circuits are composed of complex but very small SMD components, requiring thorough monitoring and verification in the production process even for comparably reliable traditional 2D PCBs. Moving to additive processes introduces a number of additional uncertainties, primarily related to the inhomogeneous results of material deposition of both structural and conductive material. Some typical defects which occurred during our experiments in the last years are summarized in Fig. 5.

Even if no actual defects occur, the surface roughness of printed objects still is inherently high, increasing the probability of defects for thin conductive traces [35].

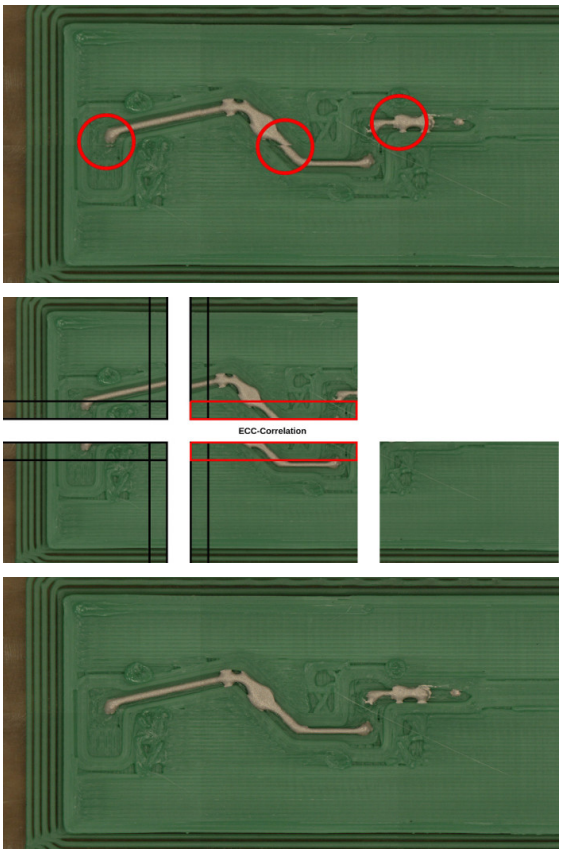

Fig. 6. Stitching of tiles into a composed layer image. **Top**: individual images as recorded are naively assembled with positioning inaccuracies highlighted in red. **Middle**: positions of tiles recorded with extended borders are corrected by pairwise correlation of overlapping regions **Bottom**: high-quality stitched layer image.

For 3D-printed electronics components and wires which are partly or entirely embedded into the structural part, the problem is even worse because visual inspection is not possible after production, let alone any attempt to repair a defect.

V. Visual Recording during the Printing Process

To obtain images with sufficient resolution and low distortion, only a small area can be covered by a single image recorded with the camera. Except for very small objects, documenting an entire layer requires to take several images which are stitched together as a first processing step. To cover only regions where material was deposited in the current layer, our tool analyzes the G-code and generates a grid with optimal coverage for each individual layer.

A resulting set of tiles for one layer is given in Fig. 6. Unfortunately, simple stitching of the tiles into one image proved to be inadequate for our belt-driven gantry systems. In many cases, backlash effects and insufficient positioning precision caused significant offsets. To reduce stitching inaccuracies, we record tiles with a certain overlap and apply correlation based image alignment on the overlapping regions [29]. New tiles are appended iteratively from bottom to top, left to right. For each new tile, the offset and correlation coefficient with the bottom and left tile are computed if they exist. The new position is the average of both offsets, weighed with the correlation coefficient to prefer corrections with higher confidence.

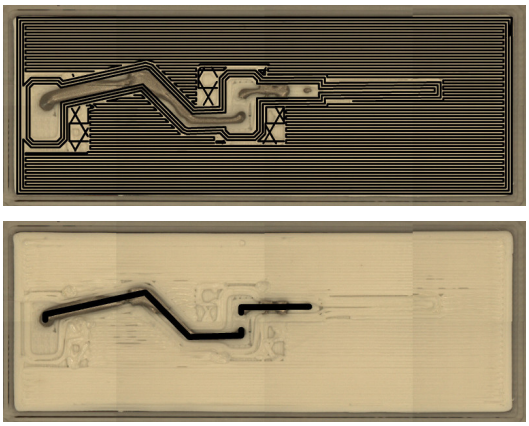

Fig. 7. Overlay of the raw image and G-code of a single layer. **Top**: all extrusions executed by the plastic extruder `T0` and **Bottom**: conductive ink lines extruded by `T1`.

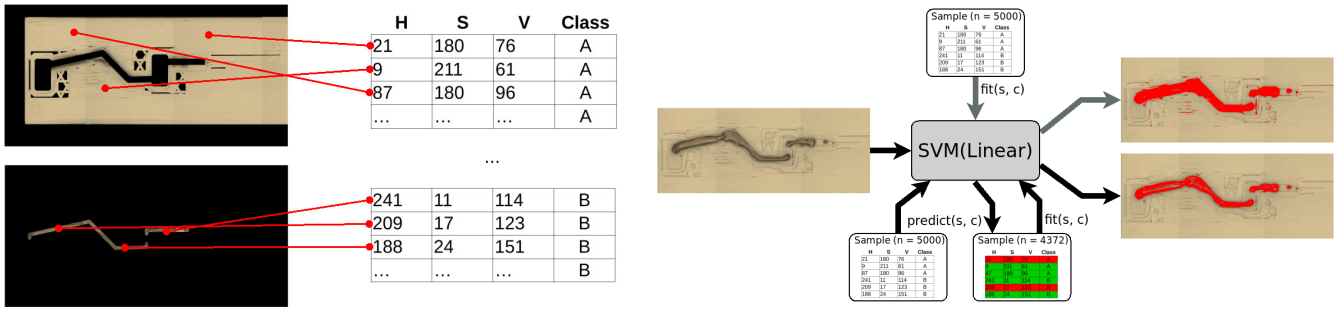

Fig. 8. SVM-based classification into plastic / conductive material. **Left**: a random subsample of plastic- and ink-pixels is extracted from the image after masking the respective tool-paths. **Right**: an SVM is trained with the labeled dataset and used to classify all pixels in the image (top). The classification accuracy is significantly improved by self-filtering the training data. Entries which do not match the prediction of the SVM are removed and the classifier is re-trained with the reduced dataset (bottom).

VI. Feature Segmentation

A reliable and accurate segmentation of regions covered with conductive ink is essential to automatically detect wire defects. Since the desired geometry of both materials is encoded in the G-code, a mask can be created by parsing all positioning commands for a particular extruder which contain a positive amount of extrusion. The mask is converted to the known image coordinate system and applied as shown in Fig. 7. This step also masks regions from previous layers, e.g. in sparse infill areas which are visible in the image.

Figure 8 left illustrates how the predetermined positions of all plastic pixels (top) and conductive ink pixels (bottom) are identified in the image by inverting the previously generated masks. Since each image typically contains several thousand pixels in each dimension, only a random subsample is extracted for each extruder to reduce the amount of data. Figure 9 clearly indicates that even a simple linear separation is sufficient to classify pixels based on their color values. The resulting dataset contains an equal number of labeled data points from both classes.

In a subsequent step, a Support Vector Machine (SVM) is trained with the labeled dataset and used to classify pixels in the image into the categories *plastic* or *ink* (Fig. 8 right). For filament colors with a low distance to the ink color, a significant number of pixels is misclassified with this method (Fig. 8, top right result). This is mainly caused by incorrect labels in the training data. The ink extrusion frequently shows slight over- or underextrusion and deviates from the intended path due to surface tension dragging the ink to the channel boundary. Most masked areas, therefore, contain a certain amount of pixels from the opposite class. To mitigate this effect, we use the SVM to self-filter the training data. The classification is predicted for all elements of the training dataset, entries for which label and SVM prediction do not match are removed. The SVM is then re-trained on the filtered dataset, yielding a clearly improved classification result (Fig. 8, right bottom).

To verify the classification step, we printed a set of otherwise identical test objects with different plastic filament colors (Fig. 10). All colors with sufficient distance to gray showed satisfying results. For very similar colors (gray), reliable recognition becomes increasingly hard, even for humans.

VII. Defect Detection

In a final analysis step, interruptions and strong deviations of the extrusion traces are automatically detected before printing the next layer. The test is implemented as a positive-

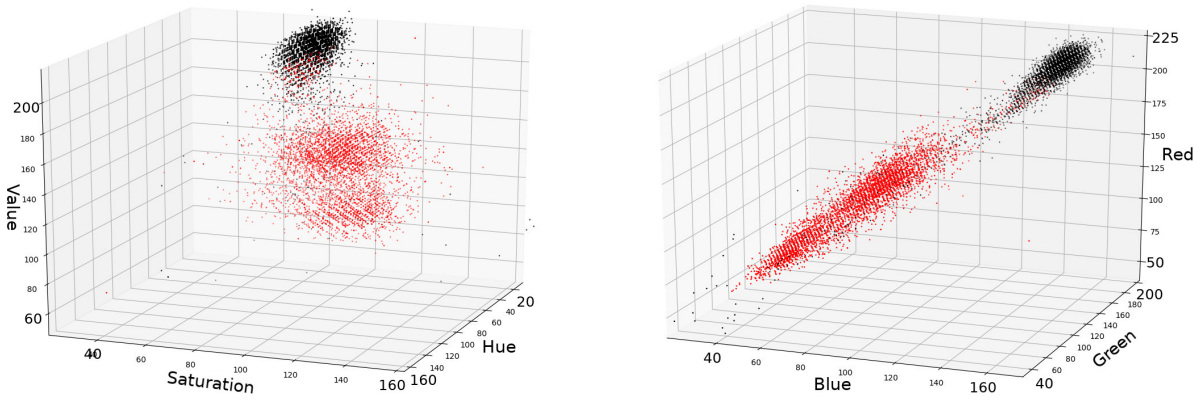

Fig. 9. Distribution of pixels in HSV (**left**) and BGR (**right**) color space. Black data points represent pixels from regions masked as plastic based on the G-code information, red data points where masked as conductive ink. Note that some pixels are misclassified due to over / unterextrusion of conductive material.

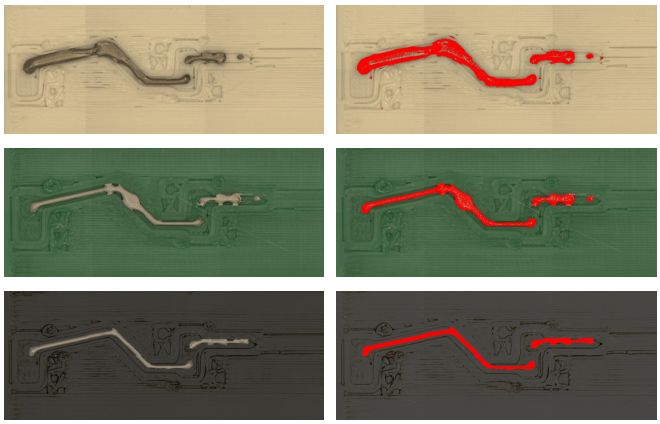

Fig. 10. Successful verification of the ink segmentation algorithm with different filament colors.

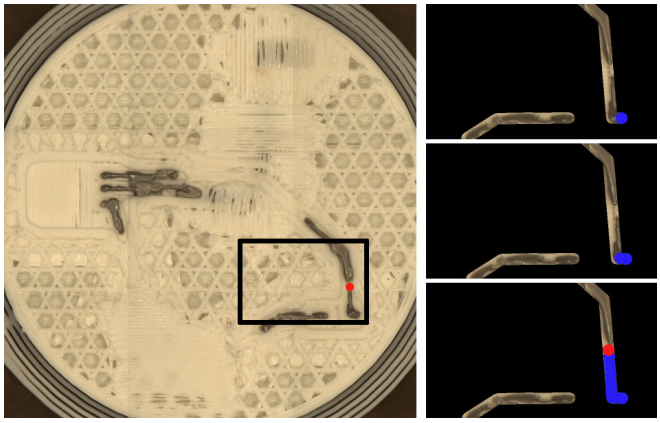

Fig. 11. A circular sliding window detector (blue), traversing the first ink extrusion line (top to bottom).

coverage, sliding window detector as illustrated in Fig. 11. A circular template, matching the extrusion diameter d_e is moved along the intended ink-extrusion lines extracted from the G-code. The template is shifted by $d_e/2$ for each iteration step. If the ratio of pixels classified as ink vs. plastic falls below a threshold ε, the region covered by this template is flagged as *defect* (red markers in Fig. 11 and 12).

VIII. Evaluation

To evaluate the performance of the defect detection pipeline, and to test the integration into the printing process and the effect on execution time, we printed a series of test objects. Five specimen with different filament colors and object shapes where manufactured with a total number of 20 layers containing conductive traces. The syringe extruder was intentionally de-calibrated to increase the probability of defects to generate relevant test data. The recorded images where inspected and labeled manually, and then compared to the automatic detection results. All disruptions and trace deviations in the evaluation dataset where successfully detected, some relevant cases with highlighted defects are provided in Fig. 12.

To be suitable as a monitoring tool, running continuously in the background during daily business in a laboratory

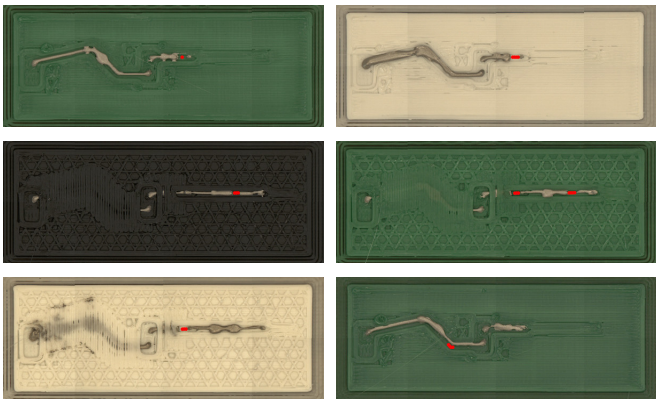

Fig. 12. Objects printed with intentionally de-calibrated syringe extruder to evaluate the detector performance. Defects automatically detected by our algorithm are highlighted in red. For this test dataset, our algorithm detected 100 % of all defects.

or production environment, the entire verification pipeline should be implemented efficiently so as to not excessively extend the overall printing-time.

Table I lists the amount of time required for the individual steps to print and verify a single layer on our test objects. The verification process (image stitching and analysis) requires approximately ∼1.0 % additional execution time per layer, which is considered reasonable. However, the image capturing step currently requires a significant amount of extra time (∼10.0 % or 4.1 s per image). This is due to positioning of the camera, followed by image capturing, cropping and import of the image on the (slow) CPU of the 3D-printer. Interleaving the printhead motion and off-loading image processing to a (much faster) PC would reduce the reported time for image capture dramatically.

TABLE I

Processing time of a single layer, broken down into the steps of the verification pipeline

	Cube		Cylinder	
Tiles	8 (2x4)		9 (3x3)	
Printing	252.0 s	87.7 %	360.0 s	89.7 %
Image capturing	33.1 s	11.5 %	37.2 s	9.3 %
Stitching	0.8 s	0.3 %	2.7 s	0.7 %
Analyzing	1.5 s	0.5 %	1.6 s	0.4 %
Sum	287.4 s		401.5 s	

IX. Conclusion and Outlook

In this work, we presented a novel approach to capture, monitor and verify printed electronics integrated into FDM-based processes. The documentation aspect, including generation of layer-by-layer high-res stitched images and their comparison to region segmentation of the G-code, are potentially also very useful for (multi-material) FDM-printing in general. In our application, conductive ink traces are identified on the images by a self-adapting segmentation algorithm. In a final step, it is verified that all intended ink traces are actually covered by ink; and the process is interrupted if defects are detected. Our tool is implemented

in a modular fashion as an Octoprint plugin and can easily be used with a wide range of 3D-printers.

Our future work will focus on the implementation of additional and more sophisticated defect detection methods. This includes a detector to identify overextrusions and short circuits, and a check for sufficient ink extrusion covering the connector footprint outline for all SMD components before placing them. Another promising approach is a connected components detector which can be used to verify both, an intact connection between two endpoints and an intact gap between to wires (two components).

The computer vision and process monitoring software described in this paper is available as open-source on Github:

https://github.com/platsch/OctoCameraDocumentation

REFERENCES

[1] E. De Nava, M. Navarrete, A. Lopes, M. Alawneh, M. Contreras, D. Muse, S. Castillo, E. Macdonald, and R. Wicker, "Three-Dimensional Off-Axis Component Placement and Routing for Electronics Integration using Solid Freeform Fabrication," *Proceedings of the 19th International Solid Freeform Fabrication Symposium*, pp. 362–369, 2008.

[2] A. J. Lopes, E. MacDonald, and R. B. Wicker, "Integrating stereolithography and direct print technologies for 3D structural electronics fabrication," *Rapid Prototyping Journal*, vol. 18, pp. 129–143, 2012.

[3] D. Periard, E. Malone, and H. Lipson, "Printing embedded circuits," *Proceedings of the International Solid Freeform Fabrication Symposium*, pp. 503–512, 2007.

[4] C. Gutierrez, R. Salas, G. Hernandez, D. Muse, R. Olivas, E. MacDonald, M. D. Irwin, R. Wicker, K. Churck, M. Newton, and B. Zufelt, "CubeSat Fabrication through Additive Manufacturing and Micro-Dispensing," *Proceedings from the IMAPS Symposium*, 2011.

[5] F. Wasserfall, D. Ahlers, N. Hendrich, and J. Zhang, "3D-Printable Electronics - Integration of SMD Placement and Wiring into the Slicing Process for FDM Fabrication," in *Proceedings of the 27th International Solid Freeform Fabrication Symposium*, Austin, 2016, pp. 1826–1837.

[6] K. B. Perez and C. B. Williams, "Combining Additive Manufacturing and Direct Write for Integrated Electronics – A Review," *Proceedings of the International Solid Freeform Fabrication Symposium*, pp. 962–979, 2013.

[7] M. Moganti, E. F., D. C.H., and T. S., "Automatic PCB inspection algorithms: a survey," *Computer Vision and Image Understanding*, vol. 63, no. 2, pp. 287–313, 1996.

[8] E. M. Taha, E. Emary, and M. Khalid, "Automatic optical inspection for PCB manufacturing: a survey," *International Journal of Scientific and Engineering Research*, vol. 5, no. 7, pp. 1095–1102, 2014.

[9] C. K. Huang, C. W. Liao, A. P. Huang, and Y. S. Tarng, "An automatic optical inspection of drill point defects for micro-drilling," *The International Journal of Advanced Manufacturing Technology*, vol. 37, no. 11, pp. 1133–1145, Jul 2008.

[10] J. Huang, D. Yang, and C. Gong, "Inspection of PCB line defects based on directionality measurements," *Circuit World*, vol. 38, no. 3, pp. 130–141, 2012.

[11] H. Rau and C.-H. Wu, "Automatic optical inspection for detecting defects on printed circuit board inner layers," *The International Journal of Advanced Manufacturing Technology*, vol. 25, no. 9, pp. 940–946, May 2005.

[12] P. M. Vitoriano and T. G. Amaral, "3D solder joint reconstruction on smd based on 2D images," *SMT Magazine*, vol. 31, pp. 82–93, 2016.

[13] P. M. Vitoriano and T. G. Amaral, "Improved pattern matching applied to surface mounting devices components localization on automated optical inspection," *World Academy of Science, Engineering and Technology, International Journal of Computer, Electrical, Automation, Control and Information Engineering*, vol. 11, no. 4, pp. 429–433, 2017.

[14] M. Chang, B.-C. Chen, J. L. Gabayno, and M.-F. Chen, "Development of an optical inspection platform for surface defect detection in touch panel glass," *International Journal of Optomechatronics*, vol. 10, no. 2, pp. 63–72, 2016.

[15] T. Wuest, C. Irgens, and K. D. Thoben, "An approach to monitoring quality in manufacturing using supervised machine learning on product state data," *Journal of Intelligent Manufacturing*, vol. 25, pp. 1167–1180, 2014.

[16] L. Lu, J. Zheng, and S. Mishra, "A layer-to-layer model and feedback control of ink-jet 3d printing," *IEEE/ASME Trans. Mechatronics*, vol. 20, pp. 1056–1068, 2015.

[17] J. Straub, "Initial work on the characterization of additive manufacturing (3d printing) using software image analysis," *Machines*, vol. 3, no. 2, pp. 55–71, 2015.

[18] M. Khanzadeh, P. Rao, R. Jafari-Marandi, B. Smith, M. Tschopp, and L. Bian, "Quantifying geometric accuracy with unsupervised machine learning: Using self-organizing map on fused filament fabrication additive manufacturing parts," *J. Manuf. Sci. Eng.*, vol. 140, p. 031011, 2017.

[19] S. Tootooni, D. A. M., R. Donovan, P. Rao, Z. Kong, and P. Borgesen, "Classifying the dimensional variation in additive manufactured parts from laser scanned three-dimensional point cloud data using machine learning approaches," *J. Manuf. Sci. Eng.*, vol. 139, p. 091005, 2017.

[20] U. Delli and S. Chang, "Automated process monitoring in 3d printing using supervised machine learning," *Procedia Manufacturing*, vol. 26, pp. 865–870, 2018.

[21] P. Sitthi-Amorn, J. E. Ramos, Y. Wangy, J. Kwan, J. Lan, W. Wang, and W. Matusik, "Multifab: A machine vision assisted platform for multi-material 3d printing," *ACM Transactions on Graphics*, vol. 34, no. 4, p. 129, 2015.

[22] R. R. Salary, J. P. Lombardi, M. S. Tootooni, R. Donovan, P. K. Rao, P. Borgesen, and M. D. Poliks, "Computational fluid dynamics modeling and online monitoring of aerosol jet printing process," *Journal of Manufacturing Science and Engineering*, vol. 139, no. 2, p. 021015, 2017.

[23] R. R. Salary, J. P. Lombardi, P. K. Rao, and M. D. Poliks, "Online monitoring of functional electrical properties in aerosol jet printing additive manufacturing process using shape-from-shading image analysis," *Journal of Manufacturing Science and Engineering*, vol. 139, no. 10, p. 101010, 2017.

[24] Y. Huang, M. C. Leu, J. Mazumder, and A. Donmez, "Additive manufacturing: current state, future potential, gaps and needs, and recommendations," *Journal of Manufacturing Science and Engineering*, vol. 137, no. 1, p. 014001, 2015.

[25] W. K. Pratt, "Correlation techniques of image registration," *IEEE Transactions on Aerospace and Electronic Systems*, vol. 3, pp. 353–358, 1974.

[26] A. Goshtasby, G. C. Stockman, and C. V. Page, "A region-based approach to digital image registration with subpixel accuracy." *IEEE Transactions on Geoscience and Remote Sensing*, vol. 3, pp. 390–399, 1986.

[27] B. Zitova and J. Flusser, "Image registration methods: a survey," *Image and vision computing*, vol. 21, no. 11, pp. 977–1000, 2003.

[28] R. Szeliski, "Image alignment and stitching: A tutorial," *Foundations and Trends in Computer Graphics and Vision*, vol. 2, no. 1, pp. 1–104, 2006.

[29] G. D. Evangelidis and E. Z. Psarakis, "Parametric image alignment using enhanced correlation coefficient maximization," *IEEE Transactions on Pattern Analysis and Machine Intelligence*, vol. 30, no. 10, pp. 1858–1865, 2008.

[30] A. Pilchak, A. Shiveley, P. Shade, J. Tiley, and D. Ballard, "Using cross-correlation for automated stitching of two-dimensional multi-tile electron backscatter diffraction data," *Journal of microscopy*, vol. 248, no. 2, pp. 172–186, 2012.

[31] Kühling & Kühling RepRap Industrial Printer. [Accessed 18.03.2019]. [Online]. Available: https://github.com/kuehlingkuehling/RepRap-Industrial

[32] F. Wasserfall, "Topology-Aware Routing of Electric Wires in FDM-Printed Objects," in *Proceedings of the 29th International Solid Freeform Fabrication Symposium*, Austin, 2018, pp. 1649–1659.

[33] A. Ranellucci. Slic3r Project Website. [Accessed 18.03.2019]. [Online]. Available: http://slic3r.org

[34] F. Wasserfall. OctoPNP - octoprint plugin for pick and place applications, project website. [Accessed 18.03.2019]. [Online]. Available: https://github.com/platsch/OctoPNP

[35] D. Espalin, D. W. Muse, E. MacDonald, and R. B. Wicker, "3D printing multifunctionality: Structures with electronics," *International Journal of Advanced Manufacturing Technology*, vol. 72, pp. 963–978, 2014.